Catal Lett (2008) 121:19–23
DOI 10.1007/s10562-007-9313-4

Electrochemical Partial Oxidation of Methane in Solid Oxide Fuel Cells: Effect of Anode Reforming Activity

Manoj R. Pillai · David M. Bierschenk · Scott A. Barnett

Received: 27 August 2007 / Accepted: 15 October 2007 / Published online: 30 October 2007

Abstract Direct-methane solid oxide fuel cells were used to produce electricity and syngas. During initial operation at 750 °C, the cells produced 0.9 W/cm^2 and ≈90% methane conversion to syngas at a rate of 30 sccm/cm^2. However, the methane conversion decreased continuously over the first 30–40 h of operation, even though the solid oxide fuel cells (SOFC) electrical performance was stable. An additional catalyst layer on the anode yielded more stable methane conversion to syngas.

Keywords Solid oxide fuel cells (SOFC) · Electrochemical partial oxidation (EPOx) · Syngas · Methane · Ni-YSZ

1 Introduction

Direct-methane solid oxide fuel cells (SOFCs) can produce syngas by reacting methane with oxygen transported across the electrolyte, a process termed electrochemical partial oxidation (EPOx) [1–7]. Syngas is an important precursor to hydrogen and synthetic liquid chemicals/fuels including methanol and various hydrocarbons [8–10]. Advantages/disadvantages of EPOx compared with other reforming methods have been described previously [1]. Key potential advantages are similar to those for ceramic membrane reactors: production of syngas without nitrogen dilution and reduced cost due to process intensification by combining the oxygen separation and partial oxidation steps. SOFCs have the additional advantage of producing two valuable products—syngas and electricity—which can significantly improve economics [1]. Most prior reports on EPOx have utilized SOFCs with relatively low power densities and thus low syngas production rates. Recently, high-rate production of syngas (20 sccm/cm^2) along with high electrical power density (0.7 W/cm^2) at 750 °C was demonstrated using conventional Ni-YSZ anode-supported SOFCs [1]. Stable SOFC electrical output was reported for up to 300 h, but the chemical products were not measured versus time.

In this letter, we describe detailed results on the electrical output and chemical products versus time from direct-methane anode-supported SOFCs. During the early stages of operation, the SOFC reactor product composition was nearly equal to that expected at equilibrium. However, the methane conversion and syngas production rate decreased continuously over the first 30–40 h of operation. This was explained by a rapid decrease in reforming activity that has recently been reported for Ni-YSZ anodes [11], given that the SOFC electrical performance was quite stable. Thus, an additional reforming catalyst was applied to the SOFC anode, resulting in improved product stability.

M. R. Pillai (✉) · D. M. Bierschenk · S. A. Barnett
Department of Materials Science and Engineering, Northwestern University, Evanston, IL 60208, USA
e-mail: mpillai@fctnet.com

D. M. Bierschenk
e-mail: bierschenk@northwestern.edu

S. A. Barnett
e-mail: s-barnett@northwestern.edu

Present Address:
M. R. Pillai
Functional Coating Technology LLC, 1801 Maple Avenue, Suite 5320, Evanston, IL 60201, USA

2 Experimental

The SOFCs used in this study were similar to state-of-the-art devices currently being developed world-wide, consisting of Ni-YSZ anode supports, thin YSZ electrolytes, and LSM-YSZ cathodes. The Ni-YSZ anode supported SOFCs were prepared by standard powder processing techniques. The supports were prepared by ball milling NiO (J. T. Baker) and YSZ (YSZ = 8 mol% Y_2O_3-stabilized ZrO_2, TOSOH Inc.) powder in a ratio of 1:1 by weight, with 10% starch filler and 60 mL ethanol for about 24 h. The powder was die pressed into 32 mm diameter, $\approx$1.0 mm thick pellets that were pre-fired at $\approx$1000 °C for 4 h. The pre-firing provided mechanical strength for handling and improved shrinkage matching with the YSZ electrolyte during co-firing. A NiO-YSZ (1:1 by weight) anode active layer and a thin dense YSZ electrolyte layer were deposited on the NiO-YSZ supports by screen printing, as described previously [12]. The anode/electrolyte bi-layers were fired at 1,400 °C for 4 h, yielding the desired dense YSZ microstructure. An LSM-YSZ (LSM = $La_{0.8}Sr_{0.2}MnO_3$; Praxair Specialty Ceramics) cathode layer was screen printed and then fired at 1,175 °C for 1 h, followed by a screen printed pure LSM current collector layer that was fired at 1125 °C for 1 h.

For current collection during SOFC testing, a silver grid was screen printed on top of the LSM layer. Table 1 gives details of the final fuel cell geometry. In some cases, an $\approx$50 μm thick layer of a Rh-alumina commercial (Alfa Aesar: Rhodium, 1% on alumina powder, reduced) catalyst material was painted on the free surface of the Ni-YSZ anode. The catalyst was then fired at 900 °C for 1 h in air prior to cell testing.

The SOFCs were tested in a setup that has been described elsewhere [1] and is illustrated in Fig. 1. The SOFCs were sealed/attached to alumina tubes using Ag ink. Methane fuel was supplied to the SOFC using an alumina tube with an annular disc attached to the end, forcing the fuel to flow radially across the surface of the anode before flowing out. This was previously shown to improve methane conversion [1]. The other end of the alumina tube was viton O-ring sealed using a stainless steel fixture to facilitate exhaust gas collection for analysis. Silver wire leads were attached using Ag ink to the electrodes, which previously had a Ag ink current collector grid (DAD-87, Shanghai Research Institute of Synthetic Resins, Shanghai, China) applied by screen printing.

The anodes were initially reduced from NiO to Ni in 30 sccm hydrogen while ramping the cell temperature up to 750 °C ($\approx$12 h) and then for $\approx$3 h at 750 °C. Initial electrical testing was carried out first in humidified hydrogen and then in pure dry methane. Air was supplied to the cathode at a flow rate of $\approx$150 sccm at all times. Current–voltage measurements and long-term constant-current measurements were recorded using a Keithley 2420 power supply (Keithley Instruments, Inc., Cleveland, OH). The cell characteristics in air with humidified hydrogen were similar to those reported previously for comparable anode-supported cells [13], with maximum power density of $\approx$1.1–1.2 W/cm^2 at 800 °C. Electrochemical impedance

Table 1 Cell component dimensions and porosities

SOFC component	Dimension (mm)	Porosity (%)
Ni-YSZ anode support thickness	0.8	40–50
Ni-YSZ anode active layer	0.025	25–30
YSZ electrolyte layer	0.012	$\approx$0
Cathode layer	0.05	30
SOFC cell diameter	25	–
SOFC active area	240 mm^2	–
Catalyst layer thickness (in some cells)	0.05	~50–60%

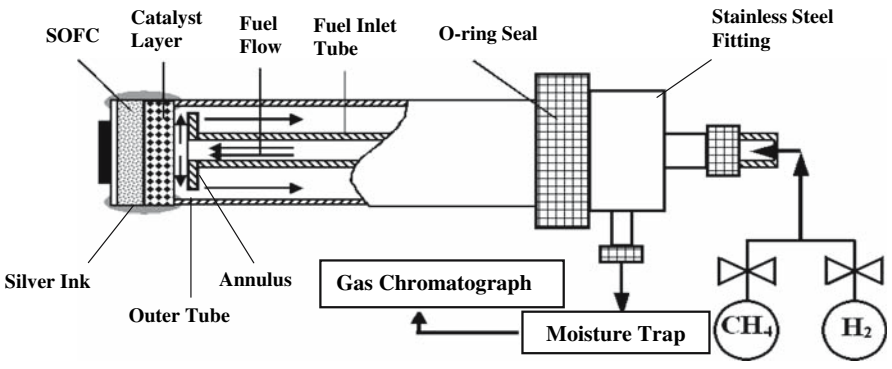

Fig. 1 Schematic diagram of the SOFC testing setup. The methane was introduced via an alumina gas feed tube (ID $\approx$ 3 mm, OD = 5 mm) with an alumina annulus (ID $\approx$ 5 mm, OD = 18.5 mm, 3 mm thick) mounted at its end. The gap between the annulus and the SOFC anode was $\approx$3 mm. The SOFC was mounted and sealed on an alumina tube (ID = 19.5 mm, OD = 25.5 mm) using Ag ink. The gas feed and mounting tubes were sealed to a stainless-steel fitting (mounted outside the testing furnace) with a viton O-ring seal

spectra were obtained using an electrochemical workstation (Zahner IM6, Germany) at frequencies ranging from 100 mHz to 100 kHz. The SOFC product gas was passed through a desiccant to remove moisture before being analyzed by an Agilent Micro Gas Chromatograph (GC) (Fig. 1). The GC was calibrated using an H_2, CH_4, CO and CO_2 gas mixture with a composition similar to that of the SOFC exhaust. The gas composition accuracy was $\approx$3–5%. Energy Dispersive Spectroscopy (EDS) was done on cross-sections of certain samples in a scanning electron microscope (SEM) (Hitachi S-3400N-II).

3 Results and Discussion

Figure 2 shows an example of the product gas composition from an SOFC operated at 750 °C versus the O^{2-}/CH_4 ratio, taken 3–4 h after the $\approx$12-h anode-reduction step was completed. The O^{2-}/CH_4 ratio was varied by changing the SOFC current and maintaining the methane flow rate constant at 20 sccm. Both the H_2 and CO contents showed a broad maximum centered at $O^{2-}/CH_4 \approx 1$, the stoichiometry of partial oxidation, with relatively low CH_4 and CO_2 content. Also shown on the plot are the predicted equilibrium gas compositions calculated using a free-energy minimization code [14]. The measured gas composition was quite close to the equilibrium prediction—the H_2 content was slightly below the prediction while the CO_2 and CH_4 contents were slightly above.

It has been suggested that SOFCs produce syngas via a two-step process [1] similar to catalytic partial oxidation of methane, where methane is oxidized to H_2O and CO_2 followed by reforming of these products with residual CH_4 to produce H_2 and CO [8]. In a SOFC, direct electrochemical oxidation of CH_4 is a possibility [4, 5, 15], but direct-methane SOFC data suggests that CH_4 oxidation on Ni-YSZ anodes is slow relative to H_2 oxidation [13, 16]. SOFC data for Ni-YSZ anodes also shows that H_2 electrochemical oxidation is faster than CO electrochemical oxidation [17, 18], and the data in Fig. 1 shows that there is plenty of H_2 in the anode compartment. Based on the above, the first reaction step should be primarily the production of H_2O by H_2 electrochemical oxidation. The second step is primarily steam CH_4 reforming, yielding H_2 and CO. The slight deviations from equilibrium in Fig. 1 can be explained by the above two-step reaction path assuming that the reforming reaction was not quite complete, yielding higher CH_4 and lower H_2 than equilibrium.

An O^{2-}/CH_4 ratio of 1.2 was previously suggested for EPOx, along with a relatively low cell voltage of 0.4 V, as a condition that maintains thermo-neutral stack operation along with high power and syngas output [1]. As shown in Fig. 2, an O^{2-}/CH_4 ratio of 1.2 was also a good condition for achieving a relatively low ($\leq$5%) un-reacted methane content, along with $\sim$6% CO_2. Note that H_2O was removed from the exhaust gas with a desiccant and hence did not appear in the product gas. The methane conversion is normally calculated using the expression:

$$\text{CH}_4 \text{ conversion } (\%) = \{([\text{CO}] + [\text{CO}_2])/([\text{CO}] + [\text{CO}_2] + [\text{CH}_4])\} \times 100, \quad (1)$$

which yields a value of $\approx$88% for $O^{2-}/CH_4 = 1.2$ at a methane flow rate of 20 sccm.

Figure 3 is a plot of the SOFC output power density and syngas production rate versus the methane flow rate and cell current; these were varied together to maintain a constant O^{2-}/CH_4 ratio of 1.2. The syngas production rate

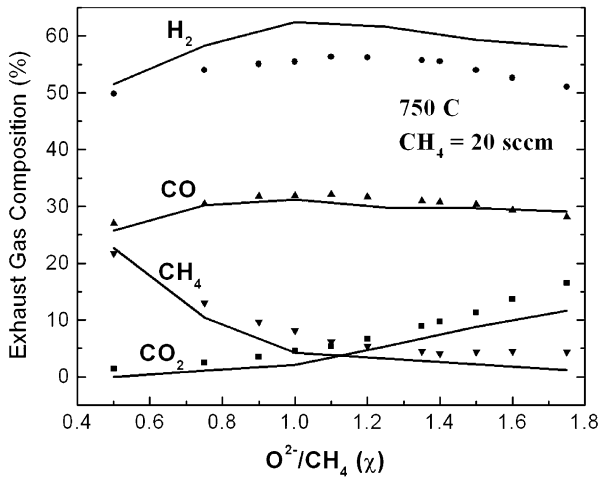

Fig. 2 Measured product gas composition (data points) and equilibrium values (curves) versus oxygen to methane ratio. Note that water vapor is removed from the exhaust using a moisture trap

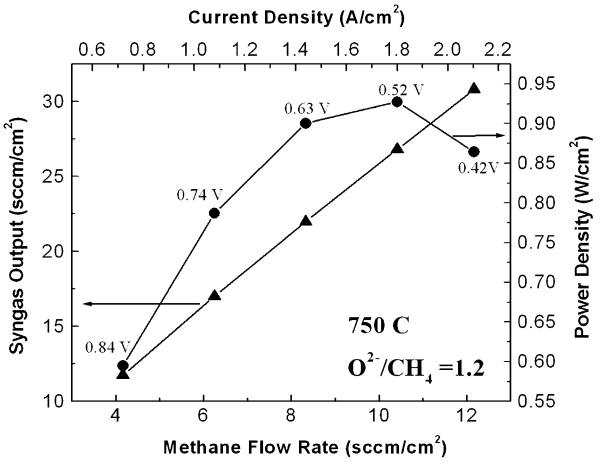

Fig. 3 Syngas output and power density versus methane flow rate (and cell current) with the ratio O^{2-}/CH_4 maintained constant at 1.2. Cell operating voltages are also given

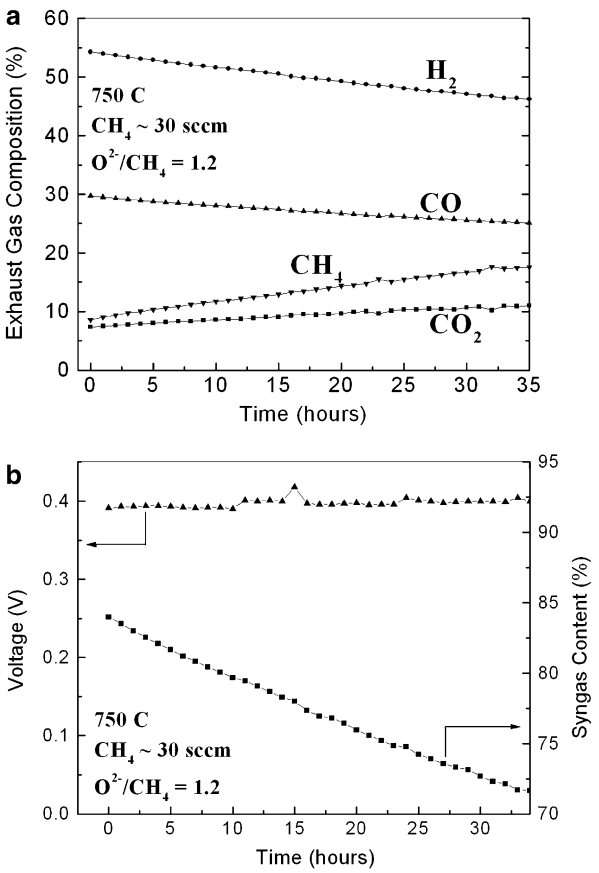

Fig. 4 Electrochemical partial oxidation (EPOx) operation with no catalyst (**a**) Change in exhaust gas composition over 35 h of continuous operation and (**b**) Measured syngas content and electrical voltage versus time from an EPOx SOFC reactor running at $J = 2.1$ A/cm^2

increased linearly with the methane inlet flow rate. The power density curve shows the usual dependence on cell current density. For a cell voltage of 0.42 V, the power density was 0.86 W/cm^2 with a syngas output of 31 sccm/cm^2. This power density is similar to state-of-the-art hydrogen-fuelled SOFCs operated at 750 °C [13, 19]. The syngas rate is comparable to membrane reactors, although these are typically operated at a higher temperature of 850–900 °C [20]. These results illustrate the efficacy of the SOFCs as dual electricity/syngas generators.

It is important to note that the data in Figs. 2 and 3 were obtained within 3–4 h after the cell had been reduced in hydrogen. The methane conversion to syngas was generally found to decrease gradually with increasing operation time. Figure 4a shows an example of this decrease, where the CH_4 content increased from ≈9% to ≈18% over 35 h, with a concomitant decrease in the H_2 and CO levels. Figure 4b shows that the SOFC voltage at a constant current density of ≈2.1 A/cm^2 was quite stable, or even increased slightly, during the course of this test. It might appear surprising that the SOFC performance remained

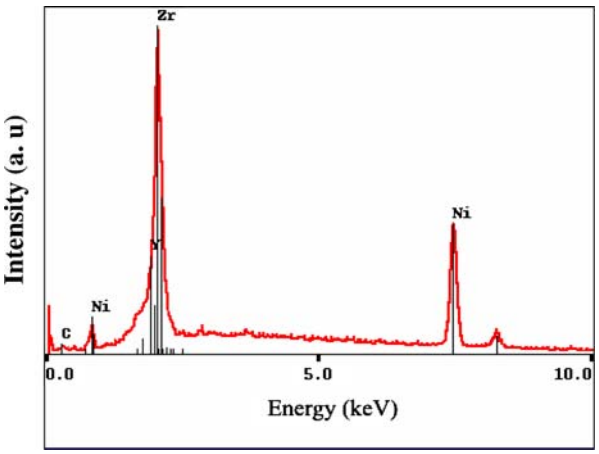

Fig. 5 Energy Dispersive Spectroscopy (EDS) spectra obtained from near the free Ni-YSZ anode surface after the cell was operated at $J = 2.1$ A/cm^2 in methane for 35 h at 750 °C

unchanged even while the gas composition in the anode was changing. However, the SOFC anode is believed to operate primarily via oxidation of H_2 (see above discussion), and the change in H_2 mole fraction in Fig. 4a is only from 54% to 46%, too small a change to significantly impact SOFC performance [17]. In any case, the decreased methane conversion was not due to a change in SOFC performance, and may be explained by a decrease in the catalytic reforming activity of the Ni-YSZ anode with time. As noted above, the Ni-YSZ activity is needed to reform CH_4 with electrochemically-produced H_2O and thereby yield the desired syngas [1].

Decreases in reforming activity with time are commonly observed for Ni-based reforming catalysts, and are typically attributed to Ni sintering and/or coking [21, 22]. Specifically, Ni-YSZ SOFC anodes have recently been shown to provide high initial reforming activity due to the formation of Ni nano-particles on YSZ surfaces, but the activity decreases substantially over tens of hours, even in

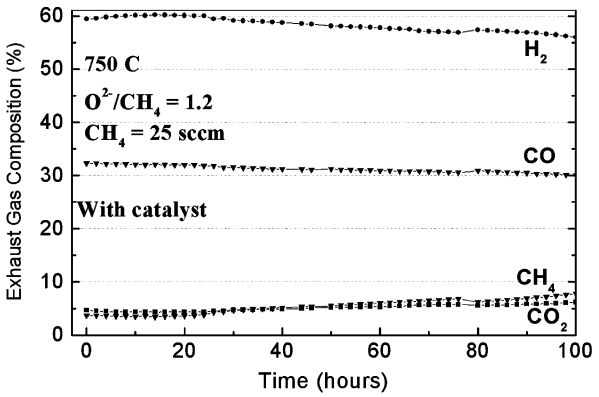

Fig. 6 The exhaust gas composition variation with time for an SOFC during EPOx operation with a Rh-alumina catalyst layer applied on the free surface of the anode

the absence of coking, due to nano-particle sintering [11]. Although the steam-to-carbon ratio was higher in that study than in the present study, the same basic effect should occur even though the Ni sintering rate may be different. The high initial reforming activity explains the nearly equilibrium conversion of methane to syngas shown in Fig. 2. The decrease in reforming activity with time yields the decrease in syngas conversion shown in Fig. 4. The present decrease in reforming activity did not appear to be related to anode coking, based on the following evidence. First, SOFC electrical performance, which has been shown to be very sensitive to coking from methane [13, 23], did not degrade with time. Second, there was no evidence of carbon on the anodes after the tests shown in Fig. 4 (and several other similar tests) as illustrated in the SEM-EDS chemical analysis shown in Fig. 5.

A cell test was carried out to determine whether the product stability could be improved by adding a Rh-alumina catalyst to the anode. Figure 6 shows that the product composition versus time was much more stable with the catalyst than without an additional catalyst (Fig. 4). While there was a slight decrease in product syngas content in this $\sim$100-h test, it was much smaller than in the shorter (35 h) no-catalyst case. More work including longer stability tests, using catalysts that are optimized for methane reforming, are needed. It seems likely that suitable catalysts can be found based on the wide range of catalysts that have been developed for reforming reactors. For example, good stability for 2,000 h at 850 °C was obtained in a ceramic membrane partial oxidation reactor with a LiLaNiO/γ-Al_2O_3 catalyst [24].

4 Summary and Conclusions

Anode-supported solid oxide fuel cells were operated directly on methane fuel with oxygen ion fluxes approximately equal to the molar methane flow rates, conditions expected to result in EPOx. During the initial several hours of SOFC operation at 750 °C, the product gas composition was nearly equal to that expected from equilibrium calculations, i.e., 88% methane conversion to syngas. The SOFC produced $\approx$0.9 W/cm^2 along with a syngas production rate of $\approx$30 sccm/cm^2. The methane conversion and syngas production rate decreased continuously over the first 30–40 h of operation, even though the SOFC electrical performance was quite stable. This resulted from decreasing Ni-YSZ anode reforming activity due to Ni nano-particle sintering, such that the syngas production rate (via methane reforming with SOFC-produced H_2O and CO_2) decreased. Initial tests showed that an added catalyst improved methane conversion stability, but more work is needed to demonstrate long-term-stable EPOx operation of SOFCs.

Acknowledgements This material is based upon work supported by the Department of Energy through the National Energy Technology Laboratory under Award Number DE-FC26-05NT42625. The authors also gratefully acknowledge Dr. Ilwon Kim of Functional Coating Technology LLC for providing the Rh-Alumina catalyst.

References

1. Zhan Z, Lin Y, Pillai M, Kim I, Barnett SA (2006) J Power Sources 161:460
2. Semin GL, Belyaev VD, Demin AK, Sobyanin VA (1999) Appl Catal A Gen 181:131
3. Ishihara T, Yamada T, Akbay T, Takita Y (1999) Chem Eng Sci 54:1535
4. Galvita VV, Belyaev VD, Demin AK, Sobyanin VA (1997) Appl Catal A Gen 165:301
5. Sobyanin VA, Belyaev VD (2000) Solid State Ionics 136:747
6. Vollmar HE, Maier CU, Nolscher C, Merklein T, Poppinger M (2000) J Power Sources 86:90
7. Zhang X, Ohara S, Chen H, Fukui T (2002) Fuel 81:989
8. Lunsford JH (2000) Catal Today 63:165
9. Rostrup-Nielsen JR (2002) Catal Today 71:243
10. Wilhelm DJ, Simbeck DR, Karp AD, Dickenson RL (2001) Fuel Process Technol 71:139
11. Strohm J, Wang Y, Roh H, Wang X, King DL (2006) III.B.10, DoE SECA review meeting
12. Von Dollen P, Barnett S (2005) J Am Ceram Soc 88:3361
13. Lin Y, Zhan Z, Liu J, Barnett SA (2005) Solid State Ionics 176:1827
14. Zhan Z, Liu J, Barnett SA (2004) Appl Catal A Gen 262:255
15. Gorte RJ, Vohs JM (2003) J Catal 216:477
16. Weber A, Sauer B, Muller AC, Herbstritt D, Ivers-Tiffee E (2002) Solid State Ionics 152–153:543
17. Jiang Y, Virkar AV (2003) J Electrochem Soc 150:A942
18. Sukeshini AM, Habibzadeh B, Becker BP, Stoltz CA, Eichhorn BW, Jackson GS (2006) J Electrochem Soc 153:A705
19. Zhao F, Virkar AV (2005) J Power Sources 141:79
20. Bouwmeester HJM (2003) Catal Today 82:141
21. Sehested J (2006) Catal Today 111:103
22. Chin YH, King DL, Roh HS, Wang Y, Heald SM (2006) J Catal 244:153
23. Lin Y, Zhan Z, Barnett SA (2006) J Power Sources 158:1313
24. Tong J, Yang W, Cai R, Zhu B, Lin L (2002) Catal Lett 78:129